MULTI-WAVELENGTH RADAR ANALYSIS OF THE LUNAR SOUTH POLAR REGION: INSIGHTS FROM MINI-RF AND DFSAR. L. M. Jozwiak[1], G. W. Patterson[1], P. Prem[1], S. S. Bhiravarasu[2], [1]Planetary Exploration Group, Johns Hopkins University Applied Physics Laboratory, Laurel, MD, USA. [2]Space Applications Centre (ISRO) Ahmedabad, India. (Corresponding author: lauren.jozwiak@jhuapl.edu).

Introduction: Questions surrounding the presence, physical form, and extent of water ice at the lunar poles have driven a large number of studies by multiple instruments over the past two decades of lunar science. Sparked by observations of suppressed neutrons in Lunar Prospector data [1, 2], and solidified by direct observations of water absorption in the LCROSS plume [3], multiple instruments onboard the LRO mission have sought to constrain the presence and distribution of water ice at the lunar poles. While several instruments have identified signatures consistent with surficial water frost [e.g. 4, 5], evidence for the persistence of these water ice deposits at depth has remained scant.

Due to the characteristic interaction between radar waves and water ice deposits [e.g. 6], several previous studies have attempted to identify the presence of water ice at the lunar south pole. Following the LCROSS impact, researchers studied both LRO/Mini-RF and Chandrayaan-1/Mini-SAR monostatic observations of the impact location in Cabeus crater; however, they did not observe the characteristic coherent backscatter effect that would be expected if spatially significant ice deposits were present [7]. It was thus concluded that, if present, the ice deposits must be smaller than the sensing wavelength of the S-band radar (~12.6 cm).

Recent numerical modeling investigations [8, 9] have investigated the relative contributions of water ice, regolith grains, and pore space to radar CPR. The initial modeling results suggest that for cases with a regolith substrate and ice grains at or below the radar sensing wavelength, there is an overall depression in observed CPR values, due to the low dielectric contrast between ice and regolith [9]. This is in direct contrast with the increase in CPR associated with relatively pure ice deposits.

Here, we examine the characteristics of the anomalously low CPR regions observed in S-band data, and extend the analysis across multiple sensing wavelengths (X-band and L-band) to further understand the nature of this signature, and possible association with water ice properties.

S-Band Analysis: Our initial analysis leverages Mini-RF S-band CPR data from a controlled polar mosaic produced by the USGS [10] in both the 0-180° (east-looking) and 180-360° (west-looking) geometries. These mosaics are fully georeferenced and co-registered to the LROC WAC 100 m global mosaic and the LOLA 512 ppd global topographic map. The mosaics provide shadow-free views of polar crater floors at a resolution of 30 m [10].

Using the methods described in [11], we isolated low-slope floor regions in 43 south polar craters with a variety of illumination conditions, including regions of permanent and seasonal shadow. From these regions, we extracted the mean CPR ±1 std. deviation.

Plots of these data revealed no distinct trend in polar crater CPR, however, the plots did reveal several locations with unusually low CPR. These data confirmed early observations by [7] that Cabeus crater hosted some of the lowest CPR values at the lunar south pole, and extended the analysis to include the craters Cabeus B, Kuhn, Sverdrup, Laveran, and unnamed crater located at 168.4°E, 88.7°S as also having anomalously low CPR values (Fig. 1).

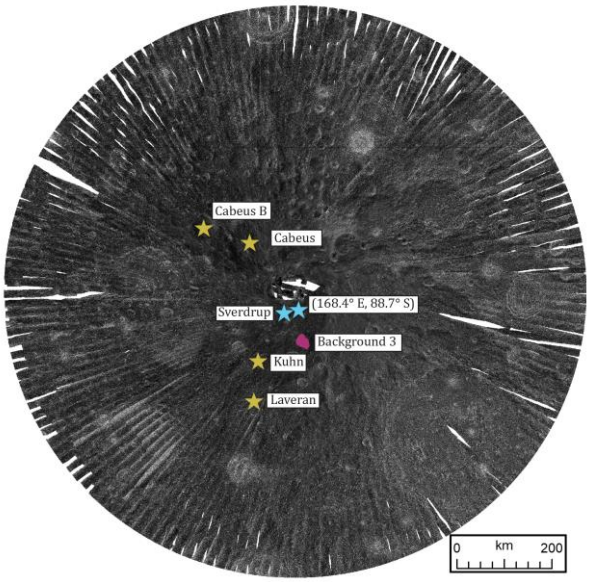

Fig. 1: Distribution of anomalously low CPR craters and regions. Blue stars indicate regions entirely in permanent shadow, yellow stars indicate a mixture of permanent and non-permanent shadow.

Physical Properties of Low CPR: Circular polarization ratio is derived by dividing the returned power in the same sense polarization by the opposite sense (SC/OC), and can therefore be interpreted as a proxy for overall roughness within the sensing depth. Increased roughness within this sensing volume can be attributed to the presence of scatterers close to the

wavelength of the incident radar [6]. The anomalously low CPR values observed in specific south polar regions, therefore, are indicative of an overall lack of roughness, both at the surface and in the shallow subsurface. In fact, the closest known CPR analog on the Moon are pyroclastic materials [11]. However, since there is no evidence for volcanic units at the lunar south pole [e.g. 12], we can instead suggest that the signature is more indicative of units with physical properties similar to pyroclastic deposits, that is exceedingly fine-grained.

Combining this physical interpretation with the results of [8], we can thus hypothesize that the regions of anomalously low S-band CPR are possible locations where regolith is mixed with pore-filling ice deposits.

Ongoing Research: While this initial result from S-band data is tantalizing, more work can be done to understand and possible constrain the nature and extent of these pore-filling ice regions. Because modeling results suggest that the suppression of CPR occurs when the size of pore-filling ice scatterers are at or below the wavelength scale of the sensing radar, the addition of multiple wavelength datasets will provide a powerful tool for understanding the scale of these deposits. Although the S-band (12.6 cm) monostatic data is the most commonly used dataset, there are 2 other polar datasets that can be used to investigate this signature: Mini-RF X-band (4.2 cm) [13] and Chandryaan-2 DFSAR L-band (24 cm) [14] data. By combining these three radar datasets, we can probe a range of ice grain sizes and distribution depths (Fig. 2).

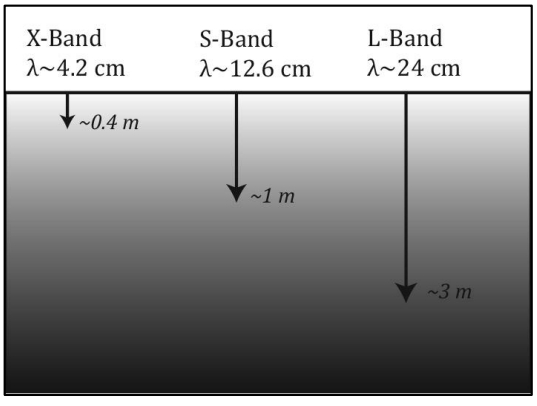

Figure 2: Comparison of radar wavelength and approximate penetration depth at the lunar south pole from LRO's Mini-RF instrument (X-band and S-band) and Chandryaan 2's DFSAR instrument (L-band).

Because controlled polar mosaics do not exist for either the X-band or L-band data, our investigations need to be more targeted than the S-band analyses described above. Instead of aggregating large averages, we instead have identified specific observations that cover 2 specific craters of interest: Cabeus and Sverdrup. Within these observations, we will apply the same slope and illumination masking described above, and will extract a range of CPR properties, both for the specific regions and also for the scene. We will then compare these results with the S-band data to investigate whether there is a wavelength dependence to the observed low CPR signature. These results will allow us to tailor our investigations for the rest of the south polar region.

References: [1] Feldman, W. C., et al. (1998) *Science, 281*, 1496-1500. [2] Lawrence, D. J., et al. (2006) *JGR Planets, 111*, E8. [3] Colaprete, A., et al. (2010) *Science 330*, 463-468. [4] Hayne, P. O., et al. (2015) *Icarus, 255*, 58-69. [5] Li, S., et al. (2018) *PNAS, 115*, 8907-8912. [6] Hapke, B. W., et al. (1993) *Science, 260*, 509-511. [7] Neish, C. D., et al. (2011) *JGR Planets, 116*, E1. [8] Prem, P., et al. (2022) SSERVI NESF [9] Fa, W., et al. (2011) *JGR Planets 116*, E3 [10] Kirk, R. L., et al. (2013) *LPSC 44*, Abstract #2920. [11] Jozwiak, L. M. et al. (2022) *LPSC 53*, Abstract #2185. [12] Fortezzo, C. M., et al. (2020) *LPSC 51*, Abstract #2760. [13] Raney, R. K., et al. (2011) *Proc. IEEE 99*, 808-823. [14] Bhiravarasu, S. S., et al. (2021) *PSJ 2*, 134.